Title

Unapodization: a method to produce laterally uniform surface acoustic waves for acoustofluidics

Journal

Journal of Micromechanics and Microengineering, 31(10)

ISSN

0960-1317

Authors

Zhang, Naiqing
Horesh, Amihai
Floer, Cécile
et al.

Publication Date

2021-10-01

DOI

10.1088/1361-6439/ac1d2d

Peer reviewed

Unapodization: A method to produce laterally uniform surface acoustic waves for acoustofluidics

Naiqing Zhang, Amihai Horesh, Cécile Floer‡, James Friend

Medically Advanced Devices Laboratory, Department of Mechanical and Aerospace Engineering, Jacobs School of Engineering and Department of Surgery, School of Medicine, University of California San Diego, La Jolla CA 92093 USA

E-mail: jfriend@ucsd.edu

4 May 2021

Abstract. Surface acoustic waves (SAW) have underpinned many acoustofluidic applications. But the typical straight, full-width interdigital transducers used to generate these waves are problematic. Fresnel diffraction of the propagating SAW causes strong nonuniformity in the wave's amplitude as it propagates across the substrate, leading to flow variations, recirculation, and peculiar wetting phenomena in fluids driven by such waves. These have led to many research projects and publications, but, ultimately, uniform fluid flow from SAW-driven streaming remains elusive. By adopting a form of apodization, the shaping of the IDT, we demonstrate the ability to produce laterally uniform SAW for acoustofluidics. *Un*like traditional apodization, which shapes the IDT to produce a desired electrical signal, this new approach—*un*apodization—instead inverts the governing equations to produce a desired spatial distribution of SAW at a defined position along the propagation direction of the SAW. Theoretical analysis and experiment demonstrate a 50% improvement in the SAW uniformity over a straight IDT for three example unapodized designs, all while maintaining the same frequency, input power, quality factor, and electromechanical coupling. The sole downside is a 50% increase in IDT area to accommodate the unapodization. A design tool is provided with tabulated unapodized IDT configurations. To illustrate the potential of unapodization in acoustofluidics, the irregular dewetting and anomalous flows of a thin fluid film induced by traditional straight IDT SAW devices is shown to become regular and uniform with the adoption of unapodized SAW devices.

Keywords: surface acoustic waves, acoustofluidics, transducer design, microelectromechanical devices

Submitted to: *J. Micromech. Microeng.*

‡ Now Assistant Professor, Université de Lorraine, CNRS, IJL, F-54000 Nancy, France.

1. Introduction

Surface acoustic waves have grown from their original use in communication systems as filters, delay lines or resonators [1] to sensors [2] and onward to become a versatile tool for quantum devices [3], optical applications [4], and, notably, acoustofluidics [5, 6]. Indeed, some have seen fit to construct a road map [7] of surface acoustic waves (SAW) to describe a few of these new uses. Most SAW devices employ a piezoelectric substrate covered by an interdigital electrode, forming an electromechanical transducer—an interdigital transducer (IDT)—first introduced by White and Voltmer in 1965 [8].

The SAW transducer design is specific to the application. The electrode length and width, material, thickness, aperture, and number of fingers define the behavior of the transducer for a selected piezoelectric substrate. Slobodnik [9] provided useful guidelines for material choice and design tradeoffs for SAW transducers in telecommunication applications many years ago. For better or worse, most of these designs devised for telecommunications [10, 11] were adopted for acoustofluidics without significant change.

Like many designs in the early 1970's, Slobodnik employed the original [8] simple, unweighted straight IDT (*see* Fig. 1(a)), still one of the most used designs today. However, there are others. By curving the electrodes [12], it becomes possible to laterally focus the acoustic energy as a focusing IDT (fIDT) in Fig. 1(b), either to a point in a circular fIDT or a line along the x axis in an elliptical fIDT, producing markedly different particle agglomeration and mixing results in sessile droplets. The single phase unidirectional transducer (SPUDT; Fig. 1(c)), of which there are many variations, including the interdigitated interdigital transducer (IIDT) [13, 14, 15], often appear in acoustofluidics as they reduce energy loss from the unused end of the IDT. However, they increase the design's complexity by halving the feature size: the narrow fingers in the illustrated version are $\lambda/8$ wide and separated by $\lambda/8$ gaps, while the wider finger is $\lambda/4$ wide. Other, less common IDT designs, including tapered IDT (TIDT) structures [16] (*see* Fig. 1(d)), chirp IDTs [17] (*see* Fig. 1(e)), and spiral IDTs [18] (*see* Fig. 1(f)), for example, are also of great interest for specific acoustofluidic applications. All of these designs, with the exception of the spiral, have parallels in SAW-based telecommunication devices.

A notable design feature of IDTs designed for telecommunications that has so far not appeared in acoustofluidics is *apodization*. In standard IDT designs (Fig. 1(a–f)), the fingers of the IDT span the width of the gap between the bus bars. In an apodized IDT design, the finger length is axially shortened along z to form a desired envelope shape along x. This produces a spatial distribution of SAW generated from an input signal, in turn producing either a broad bandwidth response [1], filtering behavior [19], or an encoding [20] effect to serve specific communications applications. Curiously, the nature of the actual electromechanical SAW generated upon the substrate from an apodized IDT has not been a focus of any of the past work to our knowledge. Because the applications for apodized IDTs have always been driven by electrical signal processing, this is probably no surprise.

Unfortunately, it is becoming clear that what best suited telecommunications

does not translate to acoustofluidics [21], including not only the IDT but also the choice of piezoelectric material and cut. Furthermore, despite some comments in the acoustofluidics community [22] that the majority of the effort lies in fluid mechanics, it is also clear that the devices used to produce acoustic waves in manipulating fluids and colloids may be significantly improved in many ways.

Notably, the intensity of the SAW across the aperture significantly varies. Depending upon where the SAW is employed, Fresnel diffraction gives rise to very different intensity

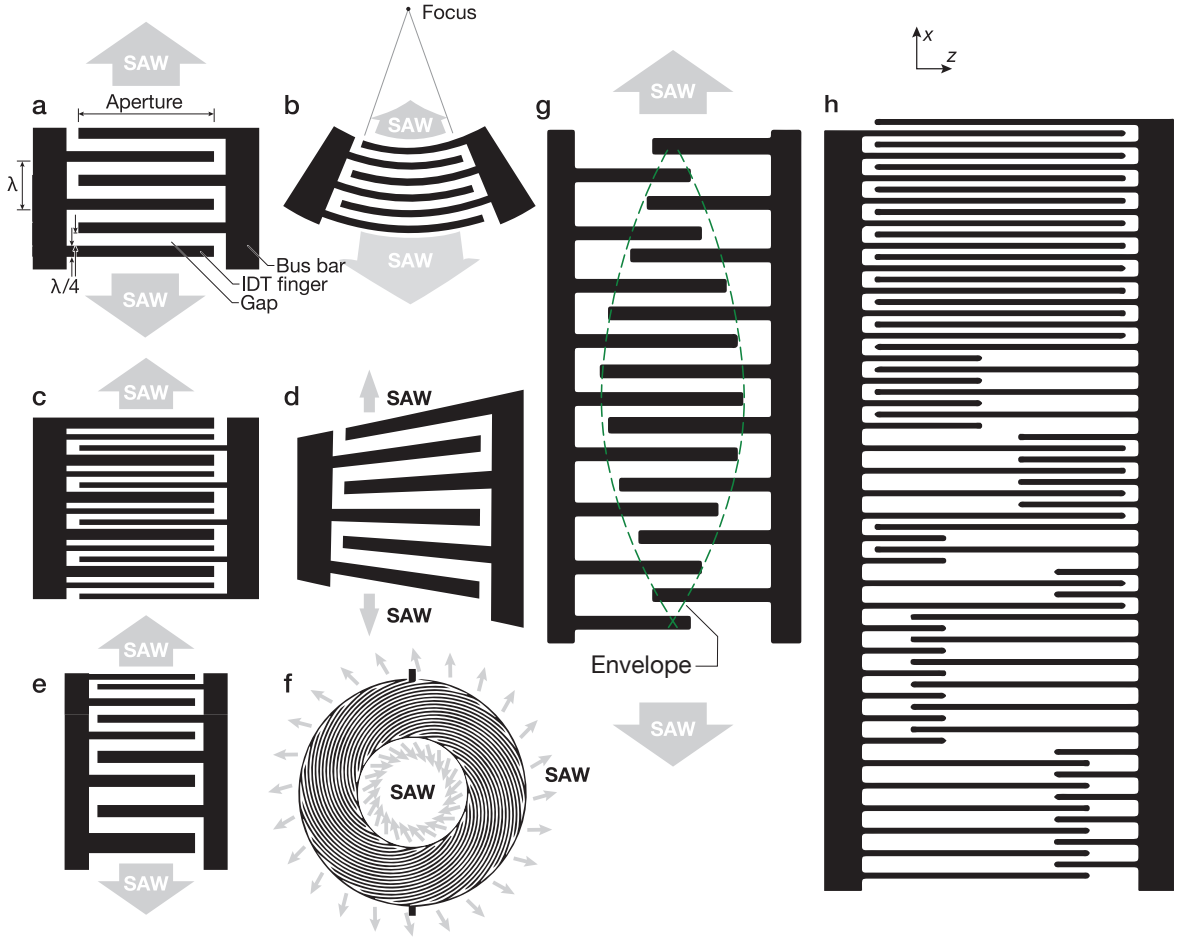

Figure 1. Interdigital electrode designs for generating SAW, including (a) the original straight, unweighted (equal gap and finger width), and full-length finger electrode IDT, which produces SAW from both ends like most IDT designs. Not shown are external reflectors that can be used to force the SAW to be unidirectional. (b) Circular focusing (fIDT), (c) single-phase unidirectional (SPUDT), (d) tapered (TIDT), (e) chirp, and (f) spiral (OSSAW) electrode patterns have been occasionally used in acoustofluidics. The SPUDT has an integrated reflector to produce SAW in only one direction, at the expense of additional complexity. (g) Apodization—shortening the IDT finger lengths according to an *envelope* function—does not appear in acoustofluidics, though it is common in telecommunications. Using an apodization method to produce a uniform lateral (along z) distribution of SAW rather than a desired electrical signal underpins the (h) *un*apodized IDT design.

distributions across the aperture, whether near-field or far-field, and none of them are uniform [23]. In a practical sense, this causes serious problems in using such devices in acoustofluidics. The induced fluid flow depends directly on the intensity of the SAW. Lateral (z axis) variations in the SAW intensity cause recirculation, flow disruption, and peculiar patterns in the advancing meniscus, among other things. Academically interpreted, these problems become "interesting phenomena in fluid transport" with papers aplenty to describe and model the behavior [24, 25, 26]. Unfortunately, the problem of nonuniform SAW causing nonuniform flow remains.

Here, we report a new approach for designing an IDT tailored to acoustofluidics. We used both theory and experiment to devise an apodized IDT. The IDT is designed to force the lateral (spatial, z-axis) distribution of the SAW amplitude to become uniform at a defined distance away from the IDT along the z axis. It is generally not possible to make the SAW amplitude laterally uniform for all z. The choice of the value of z, in significant part, defines the IDT finger patterns. Nevertheless, these finger patterns are rather *un*like the classic apodization patterns, and so we term the method *unapodization* and the IDT it produces to be *unapodized*. The design process is provided, as are several IDT designs from the process. These were fabricated and tested, and the amplitude distribution of the SAW in these designs is compared against expected values and a classic straight IDT design as a control. Further, we demonstrate the benefit of having a more uniform SAW amplitude distribution in manipulating thin fluid films as an example of the many ways such a design could benefit acoustofluidics.

2. Methods

2.1. Continuous unapodization

We consider the pressure generated at the surface of the substrate from the generation of a SAW with an amplitude distribution defined by the IDT's electrode pattern. As a SAW is generated from a standard, full-width, unweighted IDT, its pressure distribution along the axis of propagation, x, and lateral to the axis of propagation, z, is given by [23, 27]

$$p(x,z,\omega) = \sqrt{\frac{\rho_0 c k v_0}{2\pi x}} e^{i\pi/4} e^{-ikz^2/2x} \int_{-\infty}^{\infty} e^{-ikz_0^2/2x} A(z_0) e^{ik(zz_0)/x} dz_0, \tag{1}$$

where ω is the applied angular frequency; ρ_0 is the density of the medium above the substrate; c and v_0 are the sound velocity and particle vibration velocity in the solid, respectively; k is the SAW wavenumber; z_0 is a dummy variable representing the position of the IDT structure along the z axis, and $A(z_0)$ is the amplitude of the SAW at a given point z_0.

It *also* describes the presence or absence of the IDT finger along the z axis direction. Formally, the SAW amplitude at $x = 0$ linearly increases with the number of IDT finger pairs at the resonance frequency [28]. Thus, the same variable, $A(z_0)$ may be used to represent both the SAW amplitude for a given lateral position z_0 and also the number of IDT finger

pairs at that position, with only a constant as a difference between them. In fact, the *value* of $A(z_0)$ is not as important as its *distribution* in defining the IDT pattern. This is explained later when it becomes more important.

Noting the linear relationship between the generated SAW amplitude and the existence or absence of the fingers, then to have a valid solution $A(z_0)$ must be positive definite for a given value of z_0 where there is one or more IDT fingers present, and zero when there is not. This provides a means to define variable length IDT fingers. For reference, the position $x = 0, z = 0$ is located at the outer edge of the first IDT finger, at the center of the aperture. The aperture has a width, w, along the z axis.

Here we seek an IDT design with a specific amplitude distribution, and therefore an associated IDT finger distribution $A(z_0)$ to obtain a constant acoustic pressure field $p(x,z,\omega)$ across the aperture. Specifically, given a set distance away from the IDT structure of x and an applied angular frequency ω corresponding to the resonance frequency of the IDT, the acoustic pressure field $p(x,z,\omega)$ should be constant for any value of $-w/2 < z < w/2$ within the aperture. Unfortunately, it is not possible to find a function $A(z_0)$ that produces a constant pressure $p(x,z,\omega)$ for all z and x values. Later, we will be forced to choose a specific value for x, then solve for $A(z_0)$ in eqn. (1) knowing $p(x,z,\omega)$ is constant. The result will be the desired distribution of $A(z_0)$.

Before beginning this analysis, consider the classic case of straight IDTs. Typical straight IDTs (c.f., Fig. 1(a)) produce a laterally uniform SAW amplitude $A(z_0)$ across the width of the aperture, because the IDT finger produces a constant electric field across the width. The consequence, however, is that the pressure distribution generated across the width of the aperture according to eqn. (1) at the edge of the IDT, at $x = 0$, is not uniform. Furthermore, the pressure is not uniform from this point as the SAW propagates along x.

2.2. Discrete unapodization

Unfortunately, there is no closed-form solution to the inverse problem posed by eqn. (1) and the desire to find $A(z_0)$ from it. To find the amplitude and IDT finger distribution $A(z_0)$ for a uniform $p(x,z,\omega)$ at any x distance from the IDT, we laterally discretize the IDT along z into n total intervals, using $j, m \in \{1,2,\ldots,n\}$ as indices. Equation (1) becomes solvable in the j^{th} interval to describe the pressures $p_1, p_2, \ldots, p_j, \ldots, p_n$, generated by the IDT design

and consequent SAW amplitudes at $x = 0$ in each (m^{th}) interval along z, A_m:

$$\begin{aligned}
p_1 &= \Delta l \sqrt{p_0 \Gamma} \sum_{m=1}^{n} e^{i(\pi/4 - \pi\Gamma(1-m)^2 \Delta l^2)} A_m, \\
p_2 &= \Delta l \sqrt{p_0 \Gamma} \sum_{m=1}^{n} e^{i(\pi/4 - \pi\Gamma(2-m)^2 \Delta l^2)} A_m, \\
&\vdots \qquad\qquad \vdots \\
p_j &= \Delta l \sqrt{p_0 \Gamma} \sum_{m=1}^{n} e^{i(\pi/4 - \pi\Gamma(j-m)^2 \Delta l^2)} A_m, \\
&\vdots \qquad\qquad \vdots \\
p_n &= \Delta l \sqrt{p_0 \Gamma} \sum_{m=1}^{n} e^{i(\pi/4 - \pi\Gamma(n-m)^2 \Delta l^2)} A_m.
\end{aligned} \tag{2}$$

Note that for each value of $m \in \{1, 2, \ldots, n\}$, A_m is constant in the m^{th} interval, and p_j is likewise constant in the j^{th} interval. We define Δl as the width of each IDT segment along z. Assuming the total aperture of the entire IDT, w, is equally divided into n segments along z, $\Delta l = w/n$. We also define $\Gamma = (\lambda x)^{-1}$. Since A_m are used to define relative values rather than absolute values of the amplitude and associated IDT distribution in the m^{th} interval, it is possible to assume

$$p_1 = p_2 = \ldots = p_n = \Delta l \sqrt{p_0 \Gamma}.$$

Next, we choose the desired distance from the IDT along the SAW propagation direction where we want the lateral distribution of the SAW to be uniform, and define it using the variable s such that $x = s\lambda$. By solving the n equations in eqn. (2), solutions for the desired—albeit discrete—IDT intensity distribution $\{A_m\}$ ($m = 1, 2, \ldots, n$) may be found.

At resonance, the SAW amplitude at $x = 0$ and the m^{th} interval linearly increases with the number of IDT finger pairs in that interval [28]. This result from the discrete representation in eqn. (2) corresponds to the continuous case described by eqn. (1). This produces an interesting result: the number of IDT finger pairs for the m^{th} interval required to obtain a laterally uniform SAW at position x, defined as N_m, is proportional to the solution $\{A_m\}$ of eqn. (2). If the solution $\{A_m\}$ is a rational number with a common denominator for all m, then the number of IDT finger pairs required, N_m, may be defined as the numerators of A_m rounded to the nearest integers.

2.3. Aspects to consider with the unapodization method

Examples of IDT designs using this approach to produce a uniform SAW distribution across the aperture at different $x = s\lambda$ positions and for different numbers of intervals, n, are shown in Appendix A. It is important to note that as n is increased, the aperture of the IDT is more finely divided. This will improve the uniformity of the resulting acoustic pressure across the aperture. However, there are two potential problems.

First, the solution process is not entirely straightforward, even with the discrete definition provided in eqn. (2). For some choices of n and $x = s\lambda$, the solution $\{A_m\}$ may be invalid. Specifically, it may have some negative results for some of the intervals, implying that a "negative" number of IDT fingers should be used for those results. While this can potentially be accommodated by introducing the corresponding fingers into the IDT 180 degrees out of phase with respect to the overall layout, this is inconvenient and confusing. However, it is straightforward to choose another value for n and try again, and in this way we have found suitable, positive definite results for $\{A_m\}$ at many different locations x where the laterally uniform SAW is desired.

Second, as n is increased, the greater the fabrication complexity becomes. Not only does the number of intervals increase, implying that the variety of IDT finger lengths will increase, but—as will later become clear—the total number of fingers will also be increased. Combined, these two effects are important to consider in using this method.

2.4. Unapodization by example

A specific design was selected as an example: $x = 9\lambda$ and $n = 7$. By solving eqn. (2) and clearing the denominator from the members of the solution set, we have the number of required IDT finger pairs for each of the $n = 7$ intervals: N_m=16,22,14,10,14,22,16. The solution is always symmetric about the center value (when n is odd) or values (when n is even). Each value in this particular set could be divided by two to reduce the number of required finger pairs, but we choose to proceed with N_m as given.

A suitable IDT may be constructed from this result as follows. Noting the smallest number N_m for any m is ten, we require ten finger pairs for all seven (n) intervals. For $m = 1,2,3,5,6,7$, we require an additional four IDT finger pairs. Two more IDT finger pairs are required for intervals $m = 1,2,6,7$. Finally, six additional finger pairs are required for $m = 2,6$. The design requires 34 finger pairs in total. An illustration of this result is provided in Fig. 2.

2.5. Dummy fingers are important in apodization and unapodization

Apodization or unapodization of an IDT leads to a non-uniform distribution of fingers across the aperture. This is a problem because the fingers' presence on the substrate adds mass and reduces the propagation speed of the SAW they help to generate, leading to significant differences in this velocity across the aperture [29]. Since this effect is proportional to the coupling coefficient k^2_{eff}, the SAW being formed in the IDT structure will be most distorted in substrates that have large electromechanical coupling like lithium niobate [1]. In a classic apodized IDT design *without* dummy fingers (Fig. 1(g)), SAW propagating in the middle of the aperture encounters more electrode material, causing it to be slower than SAW at the edges. In the unapodized IDT design, the SAW will be fastest at the edges of the aperture and slowest at the center. This also causes transmission discrepancies as the SAW tries to propagate out of the IDT. The change in acoustic impedance from within the IDT to the bare LN across the aperture is sufficient to cause

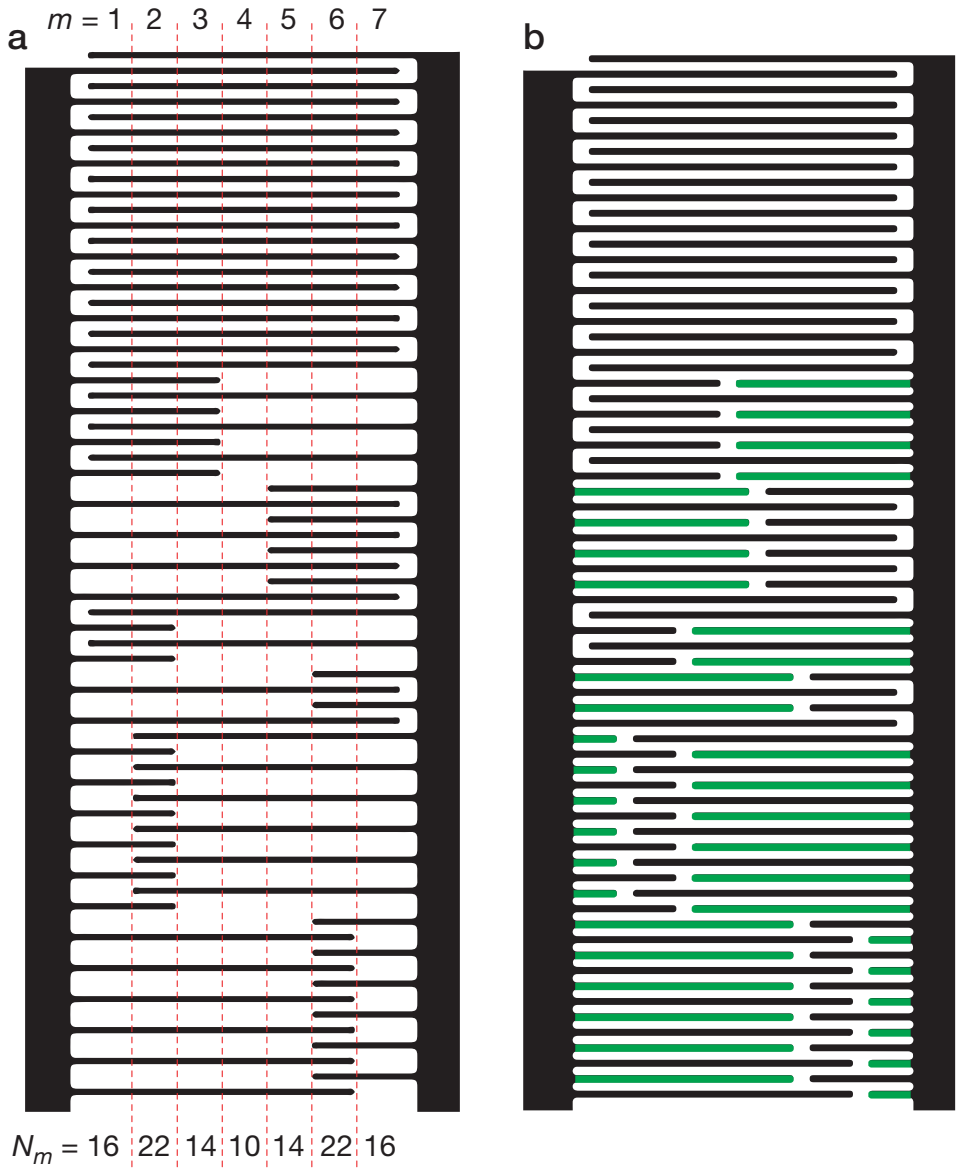

Figure 2. The results of unapodization in discrete IDT finger design for $x = 9\lambda$ and $n = 7$. The solution $\{N_m\} = \{16, 22, 14, 10, 14, 22, 16\}$ for seven intervals leads to (a) an unapodized IDT design as shown, with the interval $m \in \{1, 2, \ldots, 7\}$ indicated at top and the number of fingers required for the m^{th} interval at bottom. Dummy fingers are (b) shown in green; they are added to improve the uniformity of the wave velocity and to regularize the electrode geometry.

large SAW amplitude variations along the lateral direction z despite the unapodized IDT design.

Therefore, "dummy" fingers—additional electrode fingers connected to the opposing bus bar to avoid reflecting the propagating SAW—are used to solve this problem [30, 31]. They do not affect the electrical properties of the transducer, but significantly improve the uniformity of the SAW's propagation velocity across the aperture. Moreover, "dummy" fingers are helpful during fabrication. They regularize the pattern, reducing the risk of

over—or under—exposure issues during the lithography process.

2.6. Fabrication and testing

Using the N_m integer solutions from eqn. (2) with "dummy" fingers as shown in Fig. 2(b), we fabricated our SAW devices on double-side polished 127.86° Y-rotated cut lithium niobate (LN, Precision Micro-Optics Inc., Burlington, MA, USA), with a thickness of 500 μm, as described in ample detail elsewhere [32]. The IDTs were designed to support a wavelength of λ=100 μm (i.e., f = 40 MHz) as the minimum frequency possible for Rayleigh SAW using this LN thickness. Lower frequencies generate Lamb waves instead, which may leak energy from the back side of the wafer [33]. The double-side polished LN is normally associated with the risk of spurious bulk wave generation, and so single-side polished is preferred in many applications. Here, we anticipated the use of these devices in inverted microscopy requiring a transparent substrate—albeit birefringent. The birefringence issue may be eliminated by using a linear polarizer between the LN and objective lens.

Absorbers (Dragon Skin™, Smooth-On, Inc., Macungie, PA) were fabricated and used at both ends of the device to prevent edge reflections, triple-transit echoes, and spurious bulk waves. A SAW was generated by applying a sinusoidal electric signal to the IDT at the resonance frequency using a signal generator (WF1967 multifunction generator, NF Corporation, Yokohama, Japan) and amplifier (5U1000, Amplifier Research Corp., Souderton, Pennsylvania, USA). The electrical properties (i.e., power, current, voltage), were measured using an oscilloscope (InfiniVision 2000 X-Series, Keysight Technologies, Santa Rosa, CA). The spatiotemporal variations in the wave displacement and velocity amplitudes were measured using a scanning laser Doppler vibrometer (LDV, UHF–120SV, Polytec, Waldbronn, Germany).

3. Results

3.1. Generation of uniform SAW

Experimental results from the unapodized IDT designs showed that a laterally uniform, flat-top SAW was developed at the desired design locations for three examples. These were compared to a standard, straight IDT with full-length fingers to illustrate the value of unapodization.

The SAW amplitude distribution was measured using an LDV as it propagated from one straight and three unapodized IDT designs (*see* Fig. 3). For the straight IDT design, the SAW forms a strongly nonuniform amplitude distribution across the aperture throughout the measurement region. Evidence of this is found in the cross-section amplitude plots in Fig. 3(b–d), taken at the red lines indicated in Fig. 3(a), namely at $x = 9\lambda, 11\lambda$, and 18λ. There are two prominent peaks symmetrically placed about the weaker SAW present at the center of the aperture.

It is important to note the relation between the amplitude and pressure of the SAW after it is fully formed by the IDT and is propagating across the LN substrate surface. The

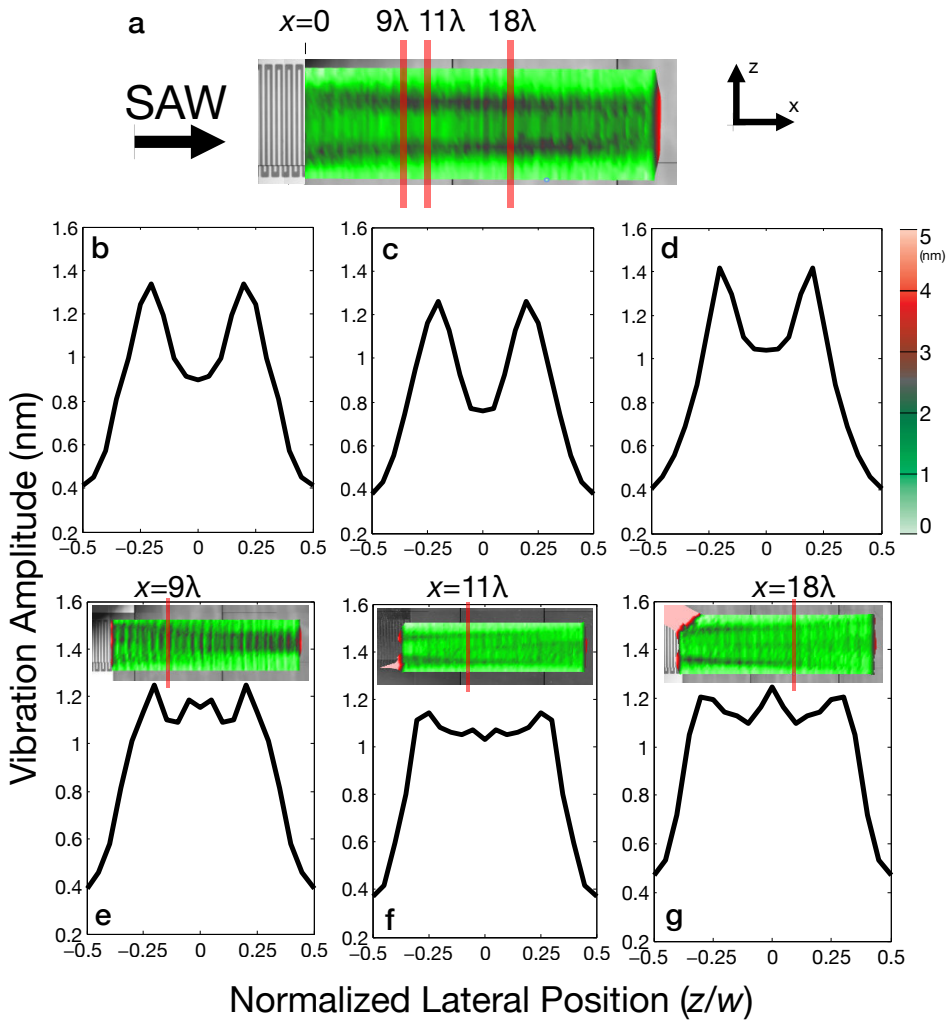

Figure 3. The SAW amplitude distribution within the IDT aperture ($-0.5w \leqslant z \leqslant 0.5w$) generated by (a) a straight IDT exhibits a nonuniform lateral distribution throughout, and also at locations (b) $x = 9\lambda$, (c) $x = 11\lambda$, and (d) $x = 18\lambda$ in plots along z. Note red lines in the (a) amplitude distribution plot and the color legend at the right of (d). Compared to these results, the three unapodized IDT devices appear to deliver a laterally uniform SAW amplitude at location (e) $x = 9\lambda$, (f) $x = 11\lambda$, (g) $x = 18\lambda$. Each is a unique IDT design produced from solving eqn. (2) with $\{x = 9\lambda, n = 7\}$, $\{x = 11\lambda, n = 7\}$, and $\{x = 18\lambda, n = 6\}$, respectively. All the devices were actuated at their designed resonance frequency of 38.3 MHz with an applied power of 520 mW. The unapodized IDT designs consistently show superior SAW amplitude uniformity along the lateral direction z at the selected design position x.

acoustic pressure $p = \rho_0 c A/\omega$ depends upon the amplitude of the SAW, A, where ρ_0 is the density of the LN and ω is the operating frequency. Crucially, this relation does not hold in the IDT where the SAW is being formed. Instead, eqns. (1) and (2) are appropriate there. Recall that we use these equations to determine the pressure distribution across the aperture at the edge of the IDT, $x = 0$, and the SAW propagates from there across the bare LN substrate.

The point is that the SAW amplitude as it propagates across the bare LN and beyond

the IDT is directly proportional to the acoustic pressure in the substrate. By driving a uniform pressure distribution from the unapodized IDT to appear at a defined location x from the IDT, one obtains a matching, uniform SAW amplitude across the aperture (along z).

To confirm this, three unapodized IDT designs, $\{x = 9\lambda, n = 7\}$, $\{x = 11\lambda, n = 7\}$, and $\{x = 18\lambda, n = 6\}$, were chosen to produce uniform SAW at these same three locations, respectively, in Fig. 3(e–g). These three designs are included among the several designs provided as examples in Appendix A. Again, an LDV was used to measure the SAW amplitude distribution as it propagated from each of these IDT designs at a resonance frequency of 38.3 MHz and an applied power of 520 mW. The red lines in Fig. 3(e–g) correspond to the $x = 9\lambda, 11\lambda$, and 18λ locations also used in the straight IDT results shown in Fig. 3(a–d). The unapodized designs produced far more uniform, flat-top SAW amplitude profiles than the straight IDT at the selected distances from the IDT. Elsewhere, the IDTs do exhibit a nonuniform SAW amplitude distribution, but it is apparent the uniformity is better than the straight IDT. This appears to support the notion that unapodization works. Improved results could likely be obtained by increasing n, the number of intervals used to define the unapodized pattern, at modest computational expense and perhaps a significant increase in fabrication effort.

The unapodization method only works for a distinct distance, x, away from the IDT. However, the change in the diffraction pattern in the far field—beyond about 10λ from the IDT—with respect to axial position x is much slower than in the near field [23]. A design chosen to produce a uniform SAW distribution across the aperture for a position x in the far field, therefore, could reasonably be expected to produce a uniform SAW distribution a greater range of the far field. Some evidence of this is seen in the SAW vibration amplitude contour plots in Fig. 3, especially in Fig. 3(f,g) for the $x = 11\lambda$ and $x = 18\lambda$ unapodized IDT designs.

3.2. Quantifying the uniformity of SAW

Next, we seek to quantify the uniformity of the SAW amplitude at the selected x locations in these three unapodized designs. The distribution of the amplitude discrepancies away from a uniform distribution in both the straight and unapodized designs is Gaussian, according to a Shapiro-Wilk test of the data for non-normal distribution, and so the standard deviation may be used. The straight IDT is expected to be the poorest performer, with a standard deviation of 0.17 nm, 0.18 nm, and 0.18 nm, respectively, at locations $x = 9\lambda$, $x = 11\lambda$, and $x = 18\lambda$. By comparison, the standard deviation for each of the three unapodized designs, respectively, was 0.07 nm, 0.04 nm, and 0.04 nm at these same locations. Using the same applied power of 520 mW at an operating frequency of 38.3 MHz, the average vibration amplitude across the IDT aperture $-w/2 < z < w/2$ was 1.10 nm, 1.01 nm, and 1.14 nm for the straight IDT at $x = 9\lambda$, $x = 11\lambda$, and $x = 18\lambda$, respectively. These values are roughly similar, indicating the absence of loss typical of SAW LN devices in air. The values are also similar to the three corresponding amplitudes for the three

unapodized designs at these three locations: 1.13 nm, 1.08 nm, and 1.16 nm for $x = 9\lambda$, $x = 11\lambda$, and $x = 18\lambda$, respectively.

Consequently, the unapodized IDT designs exhibited similar SAW amplitudes for the same input power of 520 mW but superior uniformity across the aperture at the chosen design locations from the IDT. The improvement in uniformity as defined by a reduction in the standard deviation is greater than 50%.

3.3. Changes in SAW device performance from unapodization

This uniformity of the SAW comes at a cost of additional area required to define the partial fingers present in the unapodization, of just under 50%. Compared to the twenty finger pairs in the straight IDT design, considered to be near optimal for the selected frequency and substrate [1], the unapodized designs do have more finger pairs in total: 34 finger pairs for $\{x = 9\lambda, n = 7\}$, 30 pairs for $\{x = 11\lambda, n = 7\}$, and 25 pairs for $\{x = 18\lambda, n = 6\}$§

Another consideration is the effect the unapodization has on the electromechanical coupling coefficient, k_{eff}. Here, we compute k_{eff}^2 from measurements of the resonance and antiresonance frequencies, f_{ar} for the latter, such that [34]

$$k_{\text{eff}}^2 \approx \frac{\frac{\pi f_{\text{r}}}{2 f_{\text{ar}}}}{\tan\left(\frac{\pi f_{\text{r}}}{2 f_{\text{ar}}}\right)}.$$

Consistently, $f_{\text{r}} = 38.30$ MHz while $f_{\text{ar}} = 40.44$ MHz, 39.94 MHz, 39.98 MHz, and 39.93 MHz for the straight IDT design and the unapodized IDT designs with $\{x = 9\lambda, n = 7\}$, $\{x = 11\lambda, n = 7\}$, and $\{x = 18\lambda, n = 6\}$, respectively. This produced $k_{\text{eff}}^2 = 12.39\%$, 9.73%, 9.95%, and 9.67%, respectively. The coupling performance of the unapodized designs is inferior to the straight IDT, but we must also consider the quality factor, $Q \sim \delta^{-1}$ where δ is the damping coefficient: the larger the Q the less damping present in the system. In designing an IDT, one may increase the number of finger pairs to produce a lower electromechanical coupling coefficient but greater quality factor. The performance of a SAW device depends on the product of the two [1], but before this is considered, we first determine the quality factor. There is evidence that apodization reduces the quality factor of shear horizontal SAW devices [35], leading to a more damped, broader frequency response. It may likewise happen in Rayleigh SAW devices, which could be problematic for a SAW device used in acoustofluidics.

The quality factor of the unapodized IDT was also calculated with respect to the straight IDT using the definition $Q \approx \frac{f_{\text{r}}}{\Delta f}$, where Δf is the full width at half maximum (FWHM), the measured width of the resonance peak at one-half its amplitude. This approximation is valid for $Q > 10$, certainly the case in our SAW devices as they typically have $Q \gg 10$. The quality factor is on the same order of magnitude whether or not the IDT is unapodized: $Q = 379.0$, 316.3, and 210.9 for the three unapodized designs, respectively

§ Twenty finger pairs at 40 MHz for Rayleigh SAW on LN with $\lambda = 100$ μm represents 2000 μm for the IDT along x. Every additional finger pair is 100 μm. Regardless of the aperture width (we used $w = 1$ mm for our devices), the average increase in IDT area is 48%.

optimized for uniform SAW across the aperture at $\{x = 9\lambda, n = 7\}$, $\{x = 11\lambda, n = 7\}$, and $\{x = 18\lambda, n = 6\}$ and in the same order as before. By comparison, the quality factor Q = 276.6 for the straight IDT. As expected, there is a weak increase in the quality factor roughly associated with an increase in the number of finger pairs: 20, 25, 30, and 34 finger pairs produces Q = 276.6, 210.9, 316.3, and 379.0. The 25-finger unapodized IDT design is lower, possibly because it is designed to produce a uniform SAW at $x = 8\lambda$, closer to the near field, letting the far-field SAW become quite nonuniform. It appears that unapodization may slightly reduce the quality factor, but the effect of the number of fingers in a given IDT design is much stronger, suggesting a probable means to overcome a low quality factor in a given design: increase the number of finger pairs. This can be achieved in the unapodized designs by multiplying by a suitable rational number greater than one to retain integers from the solution $\{N_m\}$.

The product Qk^2_{eff} is useful as a figure of merit, appearing in many places in the literature [36]. Once again in order, the four designs produce Qk^2_{eff} = 34.3, 36.9, 31.5, and 20.4, not a significant difference: within two (sample-size corrected) standard deviations of the mean for this small sample size of four.

3.4. Acoustofluidics

We now show the impact of a uniform SAW amplitude distribution on the generation of flow in thin liquid films. A 38.3 MHz SAW with applied power of 1.85 W interacted with a thin film of approximately 1 μL silicone oil (viscosity 20 cSt, #378348, Sigma-Aldrich, St. Louis, MO USA) pipetted onto the unapodized, $\{x = 18\lambda, n = 6\}$ IDT and a straight IDT SAW device for comparison. Figure 4 indicates the distribution of the oil wetting for the two types of devices, and notably indicates a clear difference between the two. A video of the phenomena (Supplemental Information) shows an obvious difference in the fluid wetting between the two types of devices as well. Compared to the non-uniform propagation of the fluid film due to the nonuniform SAW in the straight IDT design, the unapodized IDT exhibits a broadly uniform wetting and meniscus shape. Furthermore, the intense SAW present at the IDT center dewets the film in the straight IDT design, a feature not present in the unapodized system. This hints at the broader potential of unapodized IDT designs in producing uniform SAW and therefore uniform fluid flow useful in a majority of acoustofluidics applications.

4. Conclusion

We presented a new approach for obtaining laterally uniform SAW appropriate for acoustofluidics. Termed “unapodization”, the method is an inversion of the apodization process to produce the desired design, and targets a desired spatial distribution of mechanical motion instead of the classically useful, temporally controlled distribution of an electrical signal. This method overcomes Fresnel diffraction, namely large SAW amplitude variations across the aperture at a given distance along the SAW propagation

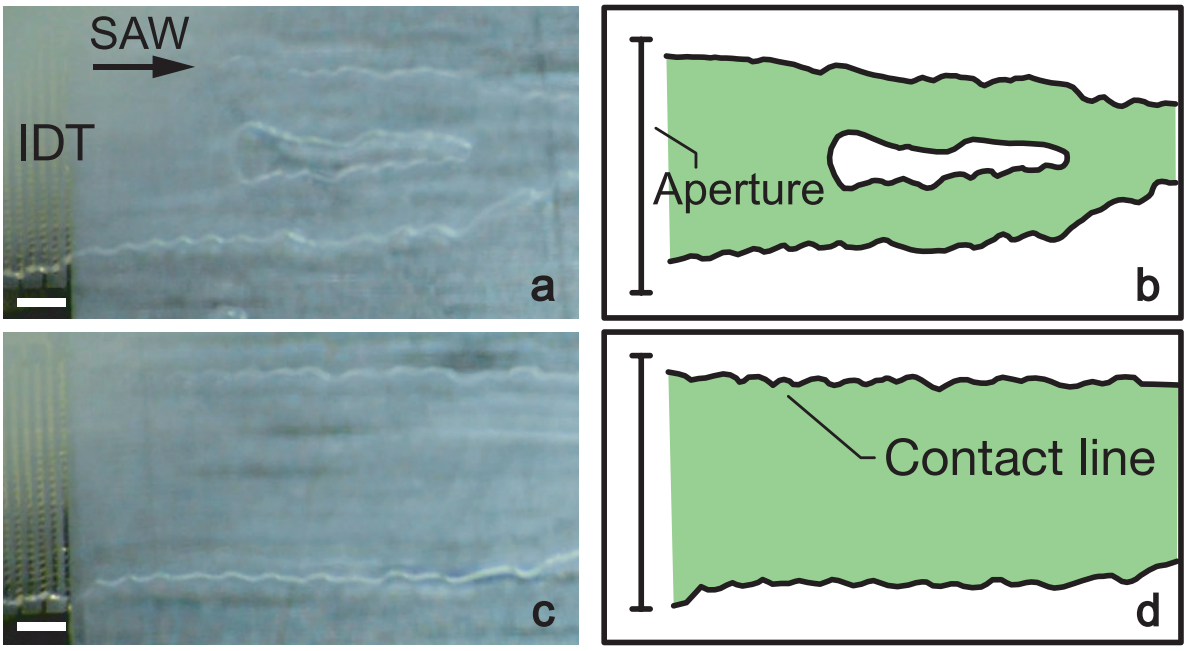

Figure 4. Manipulation of thin silicone oil film at 1.85 W and 38.3 MHz by a (a,b) straight IDT and an (c,d) unapodized IDT using a $\{x = 18\lambda, n = 6\}$ design; since both the oil and substrate are transparent, the (a,c) boundaries of the film are somewhat difficult to see in images. However, the film is (b,d) present in the green regions bound by the contact line. With a straight IDT, the oil film exhibits (a,b) nonuniform wetting with a dewetted region at the center of the aperture, exactly where the amplitude of the SAW is at its greatest. Compared this to the unapodized IDT, where the film uniformly wets the entire aperture. A comparison is perhaps more easily seen in the video provided as Supplementary Information.

axis from the IDT. Thus, the unapodized design produces laterally uniform SAW at this specific distance from the IDT. Though the full equation is not easily solvable, we presented a discretized method that is, and in fact the discretized method would likely be required to produce an IDT design that can be fabricated. The solution of the full equation would produce smoothly changing, non-integer numbers of IDT finger pairs across the aperture. These would be impossible to fabricate in current embodiments of the IDT structure.

Several unapodized IDT designs were fabricated, tested, and compared to a traditional straight-IDT design. The uniformity of the acoustic field was improved by greater than 50% while maintaining nearly the same amplitude at the same input signal power and frequency. Further, the electromechanical coupling coefficient, quality factor, and a figure of merit based on their product were found to be similar across the designs we considered, indicating the sole cost of implementing the unapodized design was the 50% additional area required to provide space for the partial IDT fingers. To prevent nonuniform SAW propagation within the IDT itself, dummy fingers were used. Finally, the unapodized IDT was applied to an acoustofluidics example: the propagation of a thin oil film across the SAW device LN substrate. Compared to the nonuniform propagation characteristics of the straight IDT design, the unapodized design produced a uniform flow across the

entire aperture ideal for acoustofluidics applications in open and, potentially, closed acoustofluidics applications.

Acknowledgements

The authors are grateful to the W.M. Keck foundation (J.F.: SERF), the National Institutes of Health (J.F.: NIH Brain Institute 1R01NS115591-01), and the University of California (J.F.: UCOP Research Grants Program Office, California HIV/AIDS Research Program) for provision of funds and facilities in support of this work. C.F. is grateful for a fellowship from the Fulbright Foundation. This work was performed at the Medically Advanced Devices Laboratory at the University of California, San Diego. Fabrication was performed in part at the San Diego Nanotechnology Infrastructure (SDNI) of UCSD, a member of the National Nanotechnology Coordinated Infrastructure, which is supported by the National Science Foundation (Grant ECCS–1542148).

Appendix A. Example solutions for unapodized IDT designs for laterally uniform surface acoustic waves

a

$s\ (x = s\lambda)$	n	Finger pair # N_m
9	7	{16,22,14,10,14,22,16}
11	5	{21,18,12,18,21}
11	7	{13,21,13,12,13,21,13}
13	5	{15,21,7,21,15}
13	7	{9,16,20,9,20,16,9}
17	5	{11,20,15,20,11}
17	7	{13,24,10,4,10,24,13}
18	5	{13,20,6,20,13}
18	6	{16,20,15,15,20,16}
18	7	{13,22,8,8,8,22,13}
18	8	{11,21,13,5,5,13,21}
19	7	{15,20,9,9,9,20,15}
20	7	{22,22,17,4,17,22,22}

b

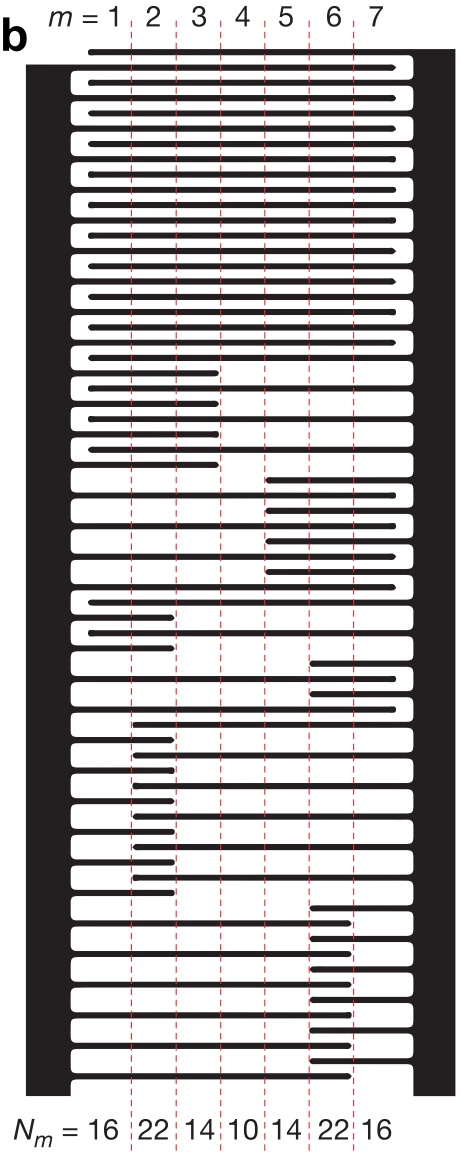

Figure A1. (a) Examples of finger pair number N_m for unapodized IDT with different vertical position $x = s\lambda$ and discrete interval number n (b) An example demonstrating the IDT finger pattern with $\{N_m\} = \{16, 22, 14, 10, 14, 22, 16\}$ by $x = 9\lambda$. Dummy fingers are not shown for clarity, but are recommended.

References

[1] Campbell C 1998 *Surface Acoustic Wave Devices for Mobile and Wireless Communications, Four-Volume Set* (Academic press)

[2] Shiokawa S and Kondoh J 2004 *Japanese Journal of Applied Physics* **43** 2799

[3] Barnes C, Shilton J and Robinson A 2000 *Physical Review B* **62** 8410

[4] Munk D, Katzman M, Hen M, Priel M, Feldberg M, Sharabani T, Levy S, Bergman A and Zadok A 2019 *Nature Communications* **10** 1–9

[5] Connacher W, Zhang N, Huang A, Mei J, Zhang S, Gopesh T and Friend J 2018 *Lab Chip* **18** 1952–1996

[6] Friend J R and Yeo L Y 2011 *Reviews of Modern Physics* **83** 647–704

[7] Delsing P, Cleland A N, Schuetz M J, Knörzer J, Giedke G, Cirac J I, Srinivasan K, Wu M, Balram K C, Bäuerle C *et al.* 2019 *Journal of Physics D: Applied Physics* **52** 353001

[8] White R M and Voltmer F W 1965 *Applied Physics Letters* **7** 314–316

[9] Slobodnik A J 1976 *Proceedings of the IEEE* **64** 581–595

[10] Matthews H 1977 *New York*

[11] Toda K and Murata Y 1977 *The Journal of the Acoustical Society of America* **62** 1033–1036

[12] Shilton R, Tan M K, Yeo L Y and Friend J R 2008 *Journal of Applied Physics* **104** 014910

[13] Winkler A, Brünig R, Faust C, Weser R and Schmidt H 2016 *Sensors and Actuators A: Physical* **247** 259–268

[14] Hodé J, Desbois J, Difilie P, Solal M and Ventura P 1995 SPUDT-based filters: Design principles and optimization *1995 IEEE Ultrasonics Symposium. Proceedings. An International Symposium* vol 1 (IEEE) pp 39–50

[15] Lewis M 1982 SAW filters employing interdigitated interdigital transducers, IIDT *1982 Ultrasonics Symposium* (IEEE) pp 12–17

[16] Mutafopulos K, Spink P, Lofstrom C D, Lu P J, Lu H, Sharpe J C, Franke T and Weitz D A 2019 *Lab Chip* **19** 2435–2443

[17] Ding X, Lin S C S, Lapsley M I, Li S, Guo X, Chan C Y, Chiang I K, Wang L, McCoy J P and Huang T J 2012 *Lab on a Chip* **12** 4228–4231

[18] Zhang N, Zuniga-Hertz J P, Zhang E Y, Gopesh T, Fannon M J, Wang J, Wen Y, Patel H H and Friend J 2021 *Lab on a Chip* **21** 904–915

[19] Morgan D 2010 *Surface acoustic wave filters: With applications to electronic communications and signal processing* (Academic Press)

[20] Vandahl T, Klett S and Buff W 1997 Multiple apodized self-correlating tapped delay line for id-tag and sensor applications *1997 IEEE Ultrasonics Symposium Proceedings. An International Symposium (Cat. No. 97CH36118)* vol 1 (IEEE) pp 349–354

[21] Zhang N, Mei J, Gopesh T and Friend J 2020 *IEEE Transactions on Ultrasonics, Ferroelectrics, and Frequency Control* **67** 2176–2186

[22] Riaud A, Baudoin M, Matar O B, Becerra L and Thomas J L 2017 *Physical Review Applied* **7** 024007

[23] Szabo T L and Slobodnik A 1973 *IEEE Transactions on Sonics and Ultrasonics* **20** 240–251

[24] Horesh A, Khaikin D, Karnilaw M, Zigelman A and Manor O 2019 *Physical Review Fluids* **4** 022001

[25] Rezk A R, Manor O, Friend J R and Yeo L Y 2012 *Nature Communications* **3** 1–7

[26] Tan M K, Yeo L and Friend J 2009 *EPL (Europhysics Letters)* **87** 47003

[27] Szabo T L 2004 *Diagnostic ultrasound imaging: inside out* (Academic Press)

[28] Manenti R 2013 *Master's Thesis, University of Milano, Milano, Italy*

[29] Tancrell R and Williamson R 1971 *Applied Physics Letters* **19** 456–459

[30] Mamishev A V, Sundara-Rajan K, Yang F, Du Y and Zahn M 2004 *Proceedings of the IEEE* **92** 808–845

[31] Smith W R, Gerard H M and Jones W R 1972 *IEEE Transactions on Microwave Theory and Techniques* **20** 458–471

[32] Mei J, Zhang N and Friend J 2020 *JoVE (Journal of Visualized Experiments)* e61013

[33] Connacher W, Zhang N, Huang A, Mei J, Zhang S, Gopesh T and Friend J 2018 *Lab on a Chip* **18** 1952–1996

[34] San Emeterio J 1997 *IEEE Transactions on Ultrasonics, Ferroelectrics, and Frequency Control* **44** 108–113

[35] Matsuda S, Miura M, Matsuda T, Ueda M, Satoh Y and Hashimoto K y 2011 *Japanese Journal of Applied Physics* **50** 07HD14

[36] Streque J, Camus J, Laroche T, Hage-Ali S, M'Jahed H, Rammal M, Aubert T, Djouadi M A, Ballandras S and Elmazria O 2020 *IEEE Sensors Journal* **20** 6985–6991